



Tailoring the structural, optical, and dielectric properties of nanocrystalline niobate ceramics for possible electronic application

Kakali Sarkar¹, Abhishek Kumar², Sharad Chandra Pandey³, Saurabh Kumar², Vivek Kumar⁴

¹Research Scholar, Department of Metallurgical and Material Engineering, Jadavpur University, Kolkata-700032, India

²Assistant Professor, Department of Electronics and Communication Engineering, Vidya Vihar Institute of Technology, Maranga, Purnea, Bihar-854303, India

³Assistant Professor, Department of Management Studies, Vidya Vihar Institute of Technology, Maranga, Purnea, Bihar-854303, India

⁴Research Scholar, Aryabhata Center for Nanoscience and Nanotechnology, Aryabhata Knowledge University, Patna 800001, Bihar, India

Email: kakaliece.nano@gmail.com

Article History

Received: 9 December 2022

Accepted: 21 January 2022

Keywords:

Magnesium niobate;
Structural analysis;
FESEM;
Band gap;
Dielectric Property

Abstract

In the past decades, magnesium niobate materials have been extensively investigated due to their exceptional dielectric characteristics at microwave frequencies and are widely employed in microwave dielectric resonators. In present research, the nanocrystalline $MgNb_2O_6$ having an orthorhombic crystal structure with $Pbcn$ space group was successfully synthesized at $1000^\circ C$ using a chemical route. X-ray diffraction (XRD), Raman spectroscopy, FESEM, impedance analyzer, and diffuse reflectance spectroscopy (DRS) were used to characterize the prepared phase. The average crystallite size, unit cell volume and the X-ray density of the prepared material were evaluated to be 52.55 nm, 407.65 \AA^3 and 4.9865 g/cm^3 , respectively. The molecular bending and stretching vibrations of metal oxide bonds were examined by Raman spectroscopy, which ranged from 232 cm^{-1} to 1007 cm^{-1} . FESEM analysis of the prepared ceramics revealed uniformly distributed grains with clear grain boundaries bearing the average grain size of 0.78 \mu m . A high direct band gap of 2.97 eV was investigated from DRS. The impedance analysis of the prepared phase revealed a decrease in the capacitance and dielectric constant between 40 Hz to 10 MHz. At 10 MHz frequency, the dielectric constant of the material was found to be 13.15. The loss tangent also displayed a systematic decrease with the increase in frequency from 40 Hz to 10 MHz.

1. Introduction

Controlling the desirable characteristics of dielectric nanomaterials has become crucial due to the rising need for novel devices, cost effective production, and excellent functionality. The investigation of certain properties, such as homogeneity, composition, grain size, etc., has focused interest on

the development of dielectric compounds. Because of its good dielectric and room-temperature luminescence capabilities, $MgNb_2O_6$ (MN_2) is thought to be a crucial material in the ceramics family. Some microwave and opto-electronic applications are rendered possible by these exceptional capabilities (Kakali et al.) In the past ten years, consider-

able research has been conducted to synthesize and examine these features for potential uses. Since the 1970s, magnesium niobite compounds have been researched to attain dependable dielectric properties (Kakali *et al.*). Norin *et al.* identified the niobate family oxides of magnesium as MgNb_2O_6 , $\text{Mg}_4\text{Nb}_2\text{O}_9$, and $\text{Mg}_5\text{Nb}_4\text{O}_{15}$ (Norin *et al.*). According to You *et al.*, the phases with stability amongst such oxides were MgNb_2O_6 and $\text{Mg}_4\text{Nb}_2\text{O}_9$ (You *et al.*). Due to its remarkable opto-electronic characteristics, magnesium niobate is widely employed in the fabrication of lead magnesium niobate, which has demonstrated advantageous for various device applications (Swartz and Shroust Joy and Sreedhar). According to earlier studies, minor amounts of $\text{Mg}_4\text{Nb}_2\text{O}_9$ or MgO are sometimes generated during the formation of MgNb_2O_6 (Sreedhar and Mitra). MN_2 phase was obtained at 1140°C using a chemical technique by Hsu *et al.* (Hsu *et al.*). Employing HF, Sarkar *et al.* produced MgNb_2O_6 and noted its good optical and dielectric abilities (Sarkar). Later, PMN (pyrochlore-free) ceramics with extremely intriguing dielectric characteristics were made using the produced MN_2 phase (Sarkar, V. Kumar, and Mukherjee). MgNb_2O_6 was also synthesized using a very productive improved combined oxide method by S. Ananta *et al.* (Ananta, Brydson, and W Thomas). We are aware that nanomaterials exhibit several intriguing features as a result of their tiny size and high surface energy. To increase the probability of enhanced ceramic implementations in microwave engineering and high optical characteristics, new production techniques are therefore required. Wet Chemical approach is one of the finest ways to create nano- MgNb_2O_6 (MN_2) ceramics as solid-state reaction process needs a lengthy heat treatment. The aim of this research is to demonstrate how to synthesise nanocrystalline MN_2 efficiently using aqueous chemicals. In addition, this study work's additional objectives for potential applications include optical investigations and dielectric analysis.

2. Materials and Method

2.1. Synthesis of MgNb_2O_6 material

With Nb_2O_5 (purity 99.99 %), sodium hydroxide (NaOH), citric acid, and analytical-grade magnesium hydroxide, a successful chemical synthesis of MgNb_2O_6 material was accomplished. After using

Nb_2O_5 as a source of niobium, Nb_2O_5 was added to NaOH. To create niobic acid solution, the mixture of glacial CH_3COOH , Nb_2O_5 , and NaOH was first stirred at 80°C for 10 hours (Sarkar and Mukherjee). The niobic acid ($\text{Nb}_2\text{O}_5 \cdot n\text{H}_2\text{O}$) solution required the addition of citric acid to create the Nb-citric acid combination. To create transparent niobium citrate stock solution, the mixture was stirred at 25°C . This stock solution was combined with $\text{Mg}(\text{OH})_2$, and the mixture of Nb^{5+} and Mg^{2+} was heated at 80°C while being constantly stirred to create a viscous liquid, which was subsequently evaporated at 100°C to produce a yellow-white substance (Ananta, Brydson, and W Thomas). The chemically processed ceramics was heat-treated at 1000°C to produce the ceramic phase of MgNb_2O_6 . The flowchart of synthesis process is shown in Fig. 1 (Kakali *et al.*).

2.2. Characterization techniques

For structural characterization, Cu K XRD (Rigaku Ultima III, 40kV, 30mA) was employed. Raman spectroscopy (WITec GmbH alpha 300RS) was used to thoroughly investigate the sample by assessing molecular bonding. FESEM (Hitachi, S-4800) was used to morphologically examine the prepared materials. EDX (INCAX sight OXFORD) was used for elemental identification. Utilizing a diffuse reflectance spectrometer (Cary 5000 Instrument), optical behaviour was investigated, and the Agilent 4294A impedance analyzer was used to assess the dielectric characteristic.

3. Results and Discussion

3.1. Analysis by XRD

XRD characterized the heat-treated MgNb_2O_6 powdered materials employing a scan rate of $5^\circ/\text{min}$ with a 2θ range from 10° to 70° degrees. With minor secondary phases of $\text{Mg}_4\text{Nb}_2\text{O}_9$ and $\text{Mg}_5\text{Nb}_4\text{O}_{15}$, prominent peaks of crystallized MgNb_2O_6 were seen in Figure 2 XRD spectra of the MgNb_2O_6 phase produced by glacial acetic acid at 1000°C for 6 h. The crystal structure of MgNb_2O_6 was determined to be orthorhombic with the P b c n space group, and the crystalline phase was indexed with the COD ID 9012222. The diffraction planes have been ascribed as (200), (110), (111), (400), (311) (020), (411), (510), etc.

The strongest reflection was observed for (311), at $2\theta = 30.26$, among these diffraction planes. The d-spacing, lattice constants (a, b and c), the cell vol-

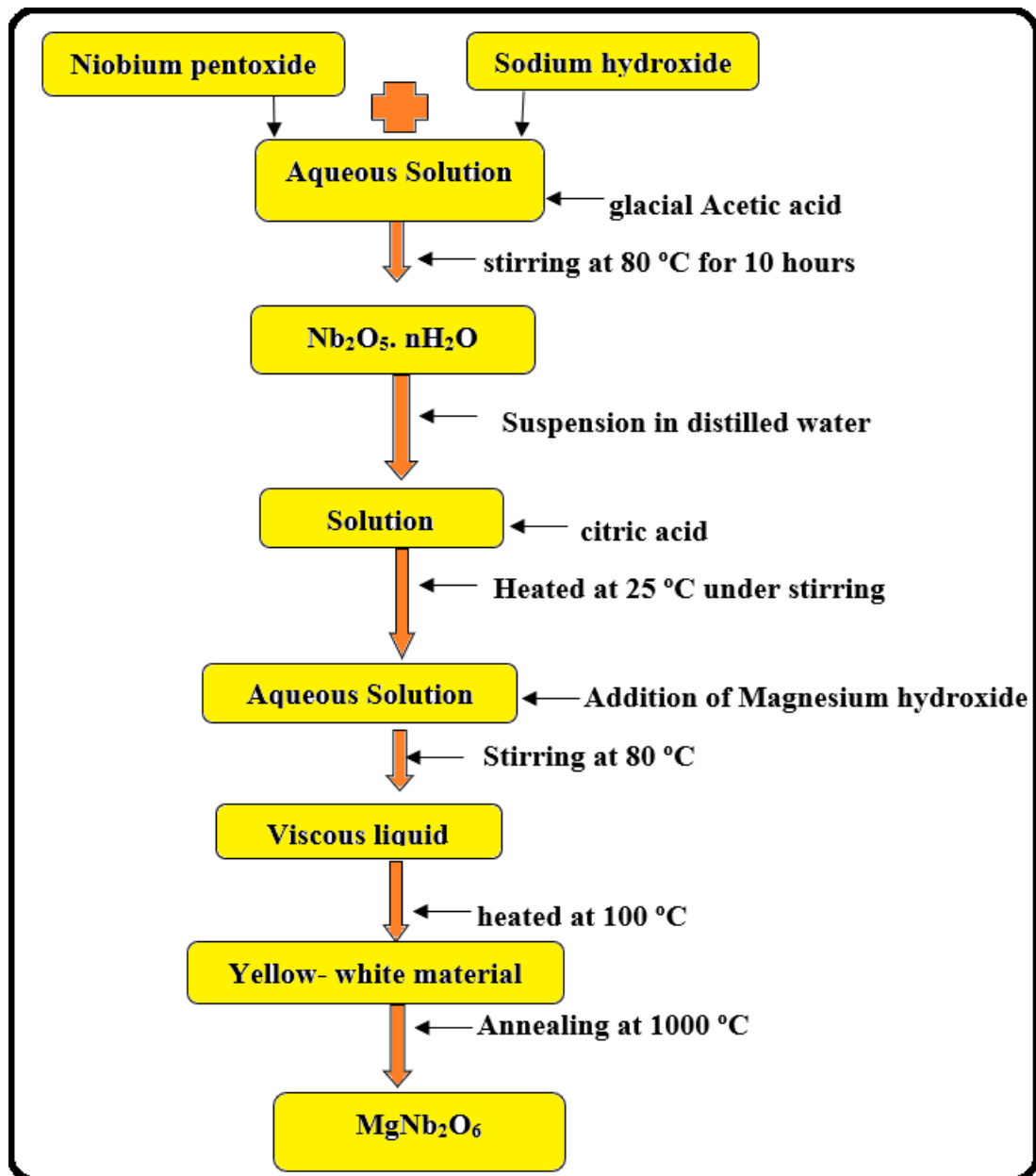


FIGURE 1. Flowchart of synthesis process

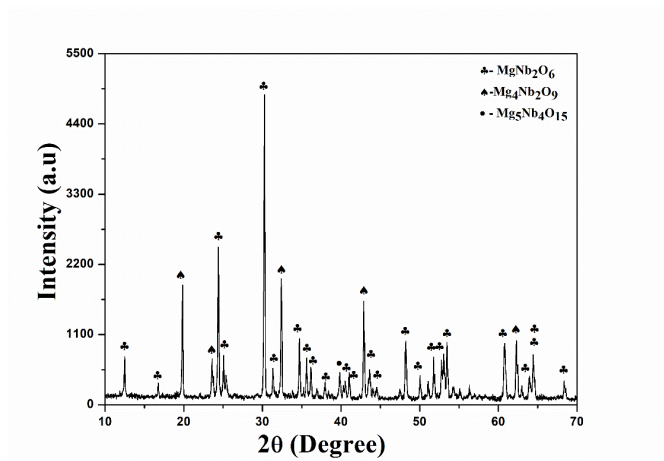


FIGURE 2. XRD spectra of MgNb_2O_6 materials

ume (V) and the X-ray density (D_x) have been calculated by the following equations:

$$n\lambda = 2d\sin\theta \quad (1)$$

$$\frac{1}{d^2} = \left(\frac{h^2}{a^2}\right) + \left(\frac{k^2}{b^2}\right) + \left(\frac{l^2}{c^2}\right) \quad (2)$$

$$V = abc \quad (3)$$

$$D_x = \frac{4M}{Na^3} \quad (4)$$

where, symbols have their usual definitions (Das et al.).

Equation 1 was used to calculate the d spacing for $2\theta = 31.34$ degrees, and the result was 2.8518 \AA . Equation 2 and prominent hkl planes were used to calculate the lattice constants. The estimated values for lattice constants a, b, and c are 14.1512 \AA , 5.7036 \AA , and 5.0507 \AA , respectively. Equation 3 was used to compute the unit cell volume, which resulted in a value of 407.65 . Equation 4 was used to determine the X-ray density (D_x), which was estimated as 4.9865 g/cm^3 . Using Scherrer's formula, $t = \frac{0.9\lambda}{\beta \cos\theta}$ (V. Kumar *et al.*), where 't' and β describe crystallite size and FWHM, the crystallite size was determined to be 52.55 nm with regard to the greatest intensity peak. Table 1 contains entire structural parameters of MgNb_2O_6 . Additionally, we prefer the W-H plot for niobate samples, which is shown in Fig. 3 and is stated in Equation 5 (Das *et al.*) to estimate the strain.

$$\beta \cos\theta = \frac{K\lambda}{D} + 4\varepsilon \sin\theta \quad (5)$$

where, symbols have their general definitions. The lattice strain (ε) for the prepared material was found to be 6.92×10^{-4} .

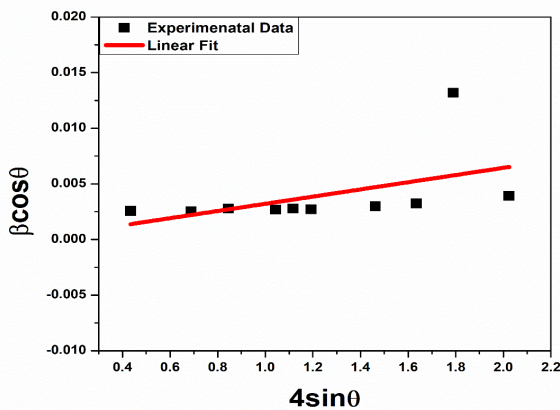


FIGURE 3. Williamson- Hall plot of MgNb_2O_6

3.2. Raman Spectroscopy

Using a confocal Raman scanning equipment, Fig. 4 shows the Raman shift of the prepared MgNb_2O_6 and lists the Raman vibration mode mappings (in cm^{-1}). Several bending and stretching vibrations of metal oxide bonds are seen in the Raman spectrum (Kakali, V. Kumar, and Mukherjee Sarkar *et al.*) in Fig. 4. The NbO_6 unit symmetric stretching vibration at 919 cm^{-1} predominated this spectrum. Nb-O bonds can be seen in the columbite

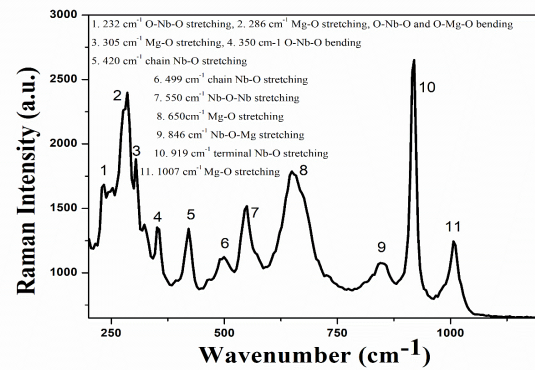


FIGURE 4. Raman shift of MgNb_2O_6

structure, where the edges and corners have been shared (Kakali, V. Kumar, and Mukherjee Sarkar *et al.*). Besides these, strong Mg-O stretching and O-Mg-O bending vibration bands are also present in Raman spectrum.

3.3. FESEM analysis

Figure 5 shows the FESEM morphology of the synthesized MgNb_2O_6 ceramics, where grain boundaries are clearly visible. Using Image J software, the mean grain size was determined to be $0.78 \mu\text{m}$. The histogram used to determine the average grain size is shown in the inset of Fig. 5. The microstructure clearly shows the merging of spherical particles.

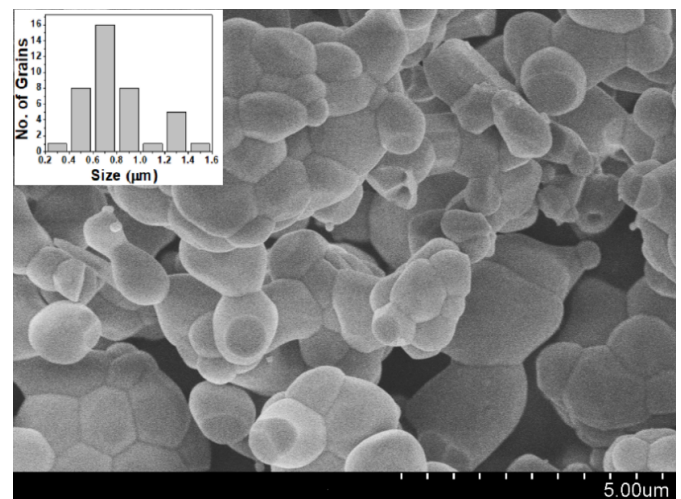


FIGURE 5. FESEM image microscope of MgNb_2O_6

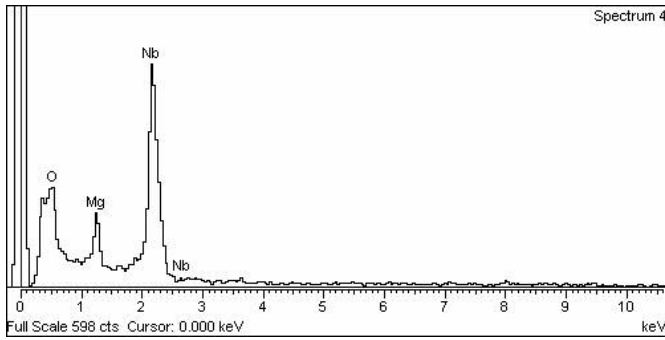
3.4. EDX analysis

The atomic peaks of only Mg, Nb, and O were seen in the EDX analysis of nanocrystals of MgNb_2O_6 , which are shown in Figure 6. This demonstrates

TABLE 1. Structural parameters obtained from XRD.

d-spacing (Å)	a(Å)	b(Å)	c(Å)	Cell volume(Å ³)	X-ray density (g/cm ³)	Crystallite size (nm)	Lattice strain (× 10 ⁻⁴)
2.8518	14.1512	5.7036	5.05.7	407.65	4.9865	52.55	6.92

the purity of the synthesized niobate compound. The estimated weight and atomic percentages of the present elements in MgNb₂O₆ are also shown in Table 2. This enables supportive evidence of the MgNb₂O₆ phase development.

**FIGURE 6.** EDX spectrum of MgNb₂O₆**TABLE 2.** EDX compositions of MgNb₂O₆

Element	Weight %	Atomic %
O K	34.20	69.42
Mg K	7.69	10.27
Nb L	58.11	20.31
Totals	100.00	

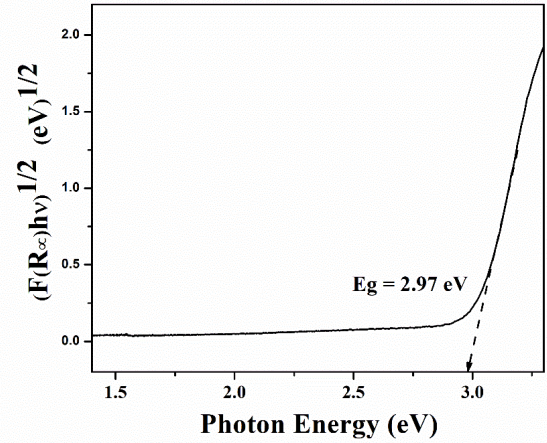
3.5. DRS analysis

In this study, direct band gap (E_g) was determined from DRS measurements spanning a 250–1500 nm wavelength range. The following equation was used to evaluate the function of reflectance (Sarkar, V. Kumar, and Mukherjee Kakali, V. Kumar, and Mukherjee Sarkar et al.):

$$F(R_\infty) = \frac{(1 - R)^2}{2R} \quad (6)$$

where, R = Reflectance and $F(R_\infty)$ = function of reflectance.

According to Fig. 7, E_g was estimated to be 2.97 eV considering the slope of the curve between $(F(R_\infty) \cdot h\nu)^{1/2}$ and $h\nu$ (Sarkar, V. Kumar, and Mukherjee Kakali, V. Kumar, and Mukherjee Sarkar et al.).

**FIGURE 7.** DRS curve of MgNb₂O₆

3.6. Dielectric Analysis

Figure 8 depicts the capacitance-frequency plot of MgNb₂O₆ pellet with applied ohmic contacts, where systematic decrease in capacitance (C) was observed with the increase in frequency. The dielectric constant ($k = \sqrt{\epsilon_r}$), inset of Fig. 8, was obtained from the value of capacitance, which also displayed a systematic decrease with the increase in frequency till 10 MHz. The relation between C and ϵ_r is expressed by the following equation:

$$C = \frac{\epsilon_0 \epsilon_r A}{d} \quad (7)$$

where notations have their general meanings (Sarkar, V. Kumar, and Mukherjee).

The loss tangent, Fig. 9 also demonstrated a decrease with the rise in frequency. k rises at low frequencies as a result of the predominance of the dipolar and interfacial polarizations (Araújo et al. Boukhari, Khalaf, and Awad Sarkar, Mukherjee, and Mukherjee). These mechanisms typically take place as a result of the porosity, oxygen vacancies, and grain structures that result in the dielectric structure's inhomogeneity. Low dielectric constant and frequency-independent stability result from the decrease in dipolar polarization and increase in electronic polarisation at high frequencies (Araújo et al.

Boukhari, Khalaf, and Awad Sarkar, Mukherjee, and Mukherjee). The dielectric constant and loss tangent have been found to be 13.15 and 0.02 at 10 MHz.

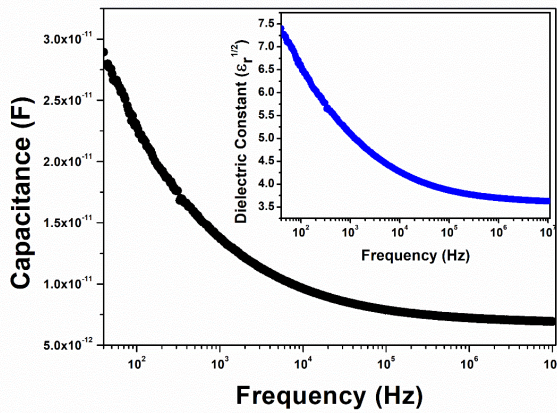


FIGURE 8. Capacitance and dielectric constant Vs Frequency of MgNb_2O_6

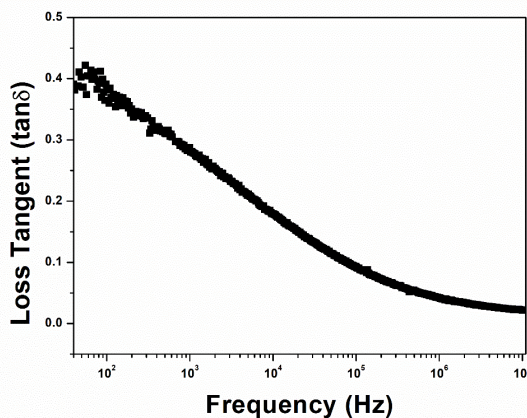


FIGURE 9. Loss Tangent Vs Frequency of MgNb_2O_6

4. Conclusions

Orthorhombic MgNb_2O_6 nanocrystalline ceramics was prepared by a chemical route, whose phase formation was identified by XRD with a crystallite size of 52.55 nm. Raman spectroscopy reveals various metal oxide bending and stretching vibrations confirming the successful synthesis of nanoceramics. FESEM analysis of the prepared ceramics revealed the merge of spherical grains with the average grain size of 0.78 μm . No elements other than Mg, Fe and O were observed from EDX analysis of MgNb_2O_6 . A high band gap of 2.97 nm was

observed, which may be due to the crystallites in nanoscale, and reflects the insulating behaviour of the prepared ceramics. Between 40 Hz and 10 MHz, the prepared phase capacitance and dielectric constant decreased, according to the impedance study. Additionally, the loss tangent showed a consistent decline from 40 Hz to 10 MHz frequency increase. The decrease in the capacitance and the dielectric constant may be due to the decrease in dipolar polarization and increase in the electronic polarization. The low dielectric loss and a high dielectric constant may facilitate its application in microwave dielectric resonators.

Acknowledgements

UGC-BSR has provided financial support for this research project. Authors acknowledge the infrastructure provided for this work by Jadavpur University, DST-Nanomission, UGC, and UGC-UPE.

References

- Ananta, Supon, Rik Brydson, and Noel W Thomas. "Synthesis, formation and Characterisation of MgNb_2O_6 Powder in a Columbite-like Phase". *Journal of the European Ceramic Society* 19.3 (1999): 355–362. [10.1016/S0955-2219\(98\)00206-4](https://doi.org/10.1016/S0955-2219(98)00206-4).
- Araújo, J C R, et al. "Tuning structural, magnetic, electrical, and dielectric properties of MgFe_2O_4 synthesized by sol-gel followed by heat treatment". *Journal of Physics and Chemistry of Solids* 154 (2021): 110051–110051.
- Boukhari, J Al, A Khalaf, and R Awad. "Structural analysis and dielectric investigations of pure and rare earth elements (Y and Gd) doped NiO nanoparticles". *Journal of Alloys and Compounds* 820 (2020): 153381–153381.
- Das, Shashank Bhushan, et al. "Structural, magnetic, optical and ferroelectric properties of Y3+ substituted cobalt ferrite nanomaterials prepared by a cost-effective sol-gel route". *Materials Science in Semiconductor Processing* 145 (2022): 106632–106632. [10.1016/j.mssp.2022.106632](https://doi.org/10.1016/j.mssp.2022.106632).
- Hsu, Cheng-Shing S, et al. "Improved high-Q microwave dielectric resonator using CuO-doped MgNb_2O_6 ceramics". *Materials Research Bulletin* 38.6 (2003): 1091–1099. [10.1016/S0025-5408\(03\)00058-8](https://doi.org/10.1016/S0025-5408(03)00058-8).

- Joy, Pattayil Alias and Krishnan Sreedhar. "Formation of Lead Magnesium Niobate Perovskite from Niobate Precursors Having Varying Magnesium Content". *Journal of the American Ceramic Society* 80.3 (1997): 770–772. [10.1111/j.1151-2916.1997.tb02896.x](https://doi.org/10.1111/j.1151-2916.1997.tb02896.x).
- Kakali, Sarkar, Vivek Kumar, and Siddhartha Mukherjee. "Synthesis, Characterization and Property Evaluation of Single Phase Mg₄Nb₂O₉ by Two Stage Process". *Transactions of the Indian Ceramic Society* 76.1 (2017): 43–49. [10.1080/0371750X.2016.1237895](https://doi.org/10.1080/0371750X.2016.1237895).
- Kakali, Sarkar, et al. "Investigation of optoelectronic properties and morphological characterization of magnesium niobate ceramics synthesized by two-stage process". *Materials Today: Proceedings* 49 (2022): 446–452. [10.1016/j.matpr.2021.02.476](https://doi.org/10.1016/j.matpr.2021.02.476).
- Kumar, Vivek, et al. "Sol-gel assisted synthesis and tuning of structural, photoluminescence, magnetic and multiferroic properties by annealing temperature in nanostructured zinc ferrite". *Materials Today: Proceedings* 47 (2021): 6242–6248. [10.1016/j.matpr.2021.05.215](https://doi.org/10.1016/j.matpr.2021.05.215).
- Norin, Rolf, et al. "Note on the Phase Composition of the MgO-Nb₂O₅ System." *Acta Chemica Scandinavica* 26 (1972): 3389–3390.
- Sarkar, K. "Synthesis, Characterization and Property Evaluation of Single Phase MgNb₂O₆ by Chemical route". *Aust. Ceram. Soc* 52 (2016): 32–40.
- Sarkar, Kakali, Vivek Kumar, and Siddhartha Mukherjee. "Synthesis and investigation of properties of nanostructured cubic PMN ceramics for possible applications in electronics". *Journal of Materials Science: Materials in Electronics* 31.17 (2020): 14314–14321. [10.1007/s10854-020-03988-2](https://doi.org/10.1007/s10854-020-03988-2).
- Sarkar, Kakali and Siddhartha Mukherjee. "Characterization and Evaluation of Property of Columbite–MgNb₂O₆ Synthesized by Chemical Route". *Journal of The Institution of Engineers (India): Series D* 97.2 (2016): 121–128. [10.1007/s40033-015-0094-4](https://doi.org/10.1007/s40033-015-0094-4).
- Sarkar, Kakali, Soumya Mukherjee, and Siddhartha Mukherjee. "Structural, electrical and magnetic behaviour of undoped and nickel doped nanocrystalline bismuth ferrite by solution combustion route". *Processing and Application of Ceramics* 9.1 (2015): 53–60.
- Sarkar, Kakali, et al. "Studies of structural, electrical and optical properties of MgNb₂O₆-Mg₄Nb₂O₉ nanocomposite for possible optoelectronic applications". *Materials Today: Proceedings* 44 (2021): 2459–2465.
- Sreedhar, K and A Mitra. "Formation of lead magnesium niobate perovskite from MgNb₂O₆ and Pb₃Nb₂O₈ precursors". *Materials Research Bulletin* 32.12 (1997): 1643–1649. [10.1016/S0025-5408\(97\)00154-2](https://doi.org/10.1016/S0025-5408(97)00154-2).
- Swartz, S L and T R Shrout. "Fabrication of perovskite lead magnesium niobate". *Materials Research Bulletin* 17.10 (1982): 1245–1250. [10.1016/0025-5408\(82\)90159-3](https://doi.org/10.1016/0025-5408(82)90159-3).
- You, Y C, et al. "Stable phases in the MgO-Nb₂O₅ system at 1250C". *Journal of Materials Science Letters* 13.20 (1994): 1487–1489. [10.1007/BF00419143](https://doi.org/10.1007/BF00419143).



© Kakali Sarkar et al. 2023 Open Access. This article is distributed under the terms of the Creative Commons Attribution 4.0 International License (<http://creativecommons.org/licenses/by/4.0/>), which permits unrestricted use, distribution, and reproduction in any medium, provided you give appropriate credit to the original author(s) and the source, provide a link to the Creative Commons license, and indicate if changes were made.

Embargo period: The article has no embargo period.

To cite this Article: Sarkar, Kakali, Abhishek Kumar, Sharad Chandra Pandey, Saurabh Kumar, and Vivek Kumar. "Tailoring the structural, optical, and dielectric properties of nanocrystalline niobate ceramics for possible electronic application." *International Research Journal on Advanced Science Hub* 05.01 January (2023): 01–07. <http://dx.doi.org/10.47392/irjash.2023.001>